# Some Performance Characteristics of Liquid Phase Spray Columns

**G. S. LADDHA**
**T. R. KRISHNAN**
**S. VISWANATHAN**
**S. VEDAIYAN**
**T. E. DEGALEESAN**
**and**
**H. E. HOELSCHER**

The A. C. College of Technology
The University of Madras
Madras 25 India

New data on residence time distribution (RTD), axial mixing, and Peclet numbers for both phases in liquid spray columns are presented.

Drop size distribution is of major interest. Continuous phase velocities affect RTD variance at high flow without appreciable effect on dispersed phase RTD variance. New correlating equations are presented.

## SCOPE

The importance of axial mixing on mass transfer has increasingly been recognized. Fluid mechanical phenomena limit column performance when mass transfer rates are high. Methods for correcting the calculated height or number of transfer units for axial mixing require a knowledge of axial mixing Peclet numbers. Earlier studies on spray columns provided insights into axial mixing but gave no useful correlations for estimating the axial mixing Peclet numbers.

New data on dispersion characteristics and flow behavior of dispersed phase droplet swarms have now been reported (Vedaiyan et al., 1972, 1974). These studies demonstrated the changing pattern of drop size distribution in the swarms (before flooding). Studies of axial mixing in the continuous phase (Kreager and Geankoplis, 1953; Mixon et al., 1967; Letan and Kehat, 1968; Henton and Cavers, 1970; Henton et al., 1973) indicate that axial mixing is primarily caused by drop movement and by carry-over of continuous phase fluid elements in the larger drop wakes. The effects of continuous and dispersed phase flow rates on axial mixing dispersion coefficients $E_c$ of the continuous phase are still uncertain. Some analyses assume uniform distribution of drop sizes for all dispersed and continuous phase flow rates, while others assume a constant mean drop size, that is, at constant dispersed phase nozzle velocity. Recent reports of Vedaiyan et al. (1972, 1974) show variations in the drop size distribution and mean drop size related to the velocity at the dispersing nozzles.

These results indicate that the continuous phase residence time distribution variance depends, to a great extent, on the same factors which affect the dispersed phase residence time distribution variance and, in addition, on the continuous phase velocity.

## CONCLUSIONS AND SIGNIFICANCE

Conclusions from this study are presented under three subheadings as follows. Data analyses follow methods outlined on Table 1 (after Levenspiel, 1972).

1. Conclusions from the dispersed phase studies. The dispersed phase RTD variance $\sigma_d^2$ varied significantly with holdup and dispersed phase velocity at the distributor nozzle $u_N$ and showed a remarkable similarity to the variation of the drop size distribution variance with nozzle velocity. (The drop size distribution was measured by photographic methods.) It seems reasonable to suggest, therefore, that the factors affecting the residence time distribution of the dispersed phase are the same as those affecting the drop size distribution.

The variance of the dispersed phase residence time distribution and axial mixing Peclet numbers were found to be best correlated with dispersed phase holdup rather than with either nozzle velocity or any modified form of the Reynolds number (see Figures 5 and 6).

2. Conclusions from the continuous phase studies. The variance of the continuous phase residence time distribution $\sigma_c^2$ was found to be a strong function of dispersed phase velocity and holdup. The continuous phase axial dispersion coefficient $E_c$ remains nearly constant at low continuous phase velocity but increases sharply at high $u_c$. Equation (2) is based on nozzle velocity and flow rate to describe the variation of the modified axial mixing Peclet numbers with operating conditions and properties.

3. Conclusions relating to the interaction of the phases. The dispersed phase residence time distribution variance, the drop size distribution, and the continuous phase residence time distribution variance were found to be strong functions of both dispersed phase and nozzle velocity (see Figures 3, 4, and 8). This may best be explained on the basis of drop size distribution studies reported earlier (Vedaiyan et al., 1972, 1974). These results were corroborated again in this present work by using the system methyl iso-butyl ketone and water. All such observations were made without coalescence or mass/heat transfer between the phases.

---

Correspondence concerning this paper should be addressed to Professor H. E. Hoelscher, Department of Chemical and Petroleum Engineering, University of Pittsburgh, Pittsburgh, Pennsylvania 15261.

The $\sigma_d^2$ minimum or the $\sigma_c^2$ maximum occurs at the critical nozzle velocity. Changes beyond this point are due to the onset of a highly nonuniform drop size distribution. Further increases in $u_N$ causes $\sigma_d^2$ to decrease, but without change in $\sigma_c^2$, as the bimodal drop size distribution region is attained.

It is reasonable to expect that $\sigma_d^2$ and $\sigma_c^2$ would behave in opposite ways to changes in nozzle velocity due to the differences in the distribution of terminal velocities in the droplet swarms as drop size distribution changes. Changing wake structures must also contribute. The low axial mixing region of the continuous phase corresponds to the same dispersed phase velocity through the nozzle, that is, the velocity at which drop uniformity is maximum. Note that the study of Henton and Cavers (1970) was confined to the region above this nozzle velocity.

Details of the experimental setup and procedure follow.

## EXPERIMENTAL

Figure 1 presents a schematic diagram of the experimental setup with details of the dye injection and sampling technique.

### Dispersed Phase Residence Time Distribution Measurements

*Procedure.* Table 2 summarized the conditions under which those data were obtained. The two output location method used for dye tracer injection in this work is thought to provide better data than methods used in previous studies.

Photographic measurements of drop sizes were made for a set of dispersed phase flow rates to obtain the variance of drop size distribution for comparison with residence time distribution results.

Because of the difficulty of measuring dye tracer concentration in the dispersed phase at two locations in the same column, as noted by Levenspiel (1972) and by Levenspiel and Bischoff (1963), two columns of different heights were used under identical conditions of operation and the response or output measured at the discharge end of the columns.

Methyl isobutyl ketone (MIBK) and distilled water were mutually saturated and then kept under constant air pressure of 5 lb/sq in. gauge in stainless steel tanks for forcing the respective liquids through the column. A microburette containing the concentrated dye tracer was kept under the same pressure. Flow rates of the dispersed and continuous phases were controlled by means of valves and orifice meters. The exact flow rates at steady column operation were measured by collecting the liquids at their outlets over known intervals of time.

First the short column was used to obtain the residence time distribution at the first location. The flow rates of dispersed and continuous phases were set at desired values. The column was operated under steady state conditions for 10 to 15 min. A pulse of tracer dye was sent through the distributor by a quick turning of the three-way stopcock so that a small quantity of, perhaps, 2 cm$^3$ (the exact quantity having been determined by preliminary tests to yield a measurable response at the interface end) was sent in under pressure as a single shot within a fraction of a second, momentarily cutting off the main dispersed phase flow and regaining the same after the pulse was sent in. Visual observation of the flow through the glass distributor during this injection period indicated that a small plug of concentrated dye solution moved from the three-way stopcock into the expanded distributor header where it was completely mixed into a uniform solution before its dispersion through the nozzles. A stopwatch was started simultaneously and samples collected in test tubes mounted on a rotating disk at the exit end of the column successively at known intervals of time. The collection of samples was continued until no trace of

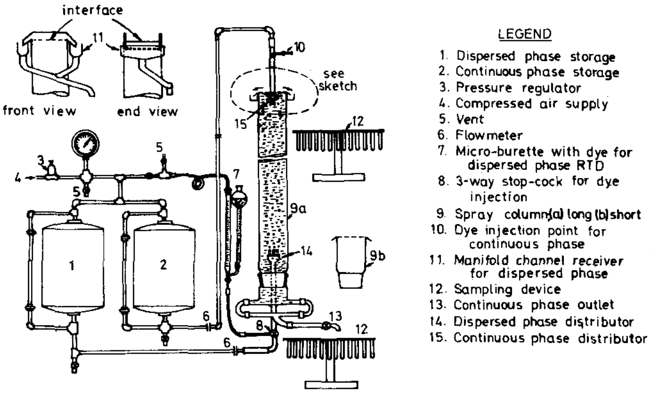

Fig. 1. Schematic diagram of experimental setup for RTD studies.

TABLE 1. REVIEW OF EQUATION USED FOR CALCULATION

| Function | Dispersed phase | Continuous phase |
|---|---|---|
| Average residence time, $\bar{t}_{\text{expt}}$ | $\bar{t}_{\text{expt}} = Lx/u_d$ | $\bar{t}_{\text{expt}} = L(1-x)u_c$ |
| First moment, $\mu_t$ | $\mu_t = \int_0^\infty t\,c(t)dt \Big/ \int_0^\infty c(t)dt$ | $\mu_t = \int_0^\infty t\,c(t)dt \Big/ \int_0^\infty c(t)dt$ |
| Mean residence time, $\bar{t}$ | $\bar{t} = (\mu_t)_2 - (\mu_t)_1$ | $\bar{t} = \mu_t$ |
| Second moment, $\sigma_t^2$ | $\sigma_t^2 = \left[\int_0^\infty t^2\,c(t)dt \Big/ \int_0^\infty c(t)dt\right] - \mu_t^2$ | $\sigma_t^2 = \left[\int_0^\infty t^2\,c(t)dt \Big/ \int_0^\infty c(t)dt\right] - \mu_t^2$ |
| Variance, $\sigma^2$ | $\sigma_d^2 = [(\sigma_t^2)_2 - (\sigma_t^2)_1]/\bar{t}^2_{\text{expt}} = (\Delta\sigma_t^2/\bar{t}^2_{\text{expt}})$ | $\sigma_c^2 = \sigma_t^2/\bar{t}^2_{\text{expt}}$ |
| Peclet number, $Pe$ | $\sigma_d^2 = 2/(Pe)_d$ | $\sigma_c^2 = \dfrac{2}{(Pe)_c} - \dfrac{2}{(Pe)_c^2}[1 - \exp\{-(Pe)_c\}$ |
| (Levenspiel, 1972; Levenspiel and Bischoff, 1963) | (based on open vessel model)<br>and<br>$(Pe)_d = u_d L/E_d$ | (based on closed vessel model)<br>and<br>$(Pe)_c = u_c L/E_c$ |

TABLE 2. SUMMARY OF EXPERIMENTAL CONDITIONS FOR RTD STUDIES

| Description | Studies of the dispersed phase | Studies of the continuous phase |
|---|---|---|
| Column | Thick walled Pyrex glass ($d_T = 5$ cm I.D.) | Same as for dispersed phase |
| Length (from nozzle tip), $L$ | 95 cm: for the long column<br>5 cm: for the short column | 94 cm (the long column alone was used) |
| Distributor: | | |
| (i) for the continuous phase | (i) A single glass tube (with a mushroom shaped cover to prevent entry of dispersed drops) | (i) Same as for dispersed phase with a side tube and 3-way stop-cock for dye entry |
| (ii) for the dispersed phase | (ii) Glass distributor head with four glass nozzles, each 2 cm long and 0.3175 cm I.D. | (ii) As for the dispersed phase |
| Setup | As in Figure 1 (note the details for dye entry and top arrangement for sample collection) | As in Figure 1 |
| Dispersed phase: | Methyl isobutyl ketone (MIBK) (saturated with the continuous phase liquid) | 1. MIBK (saturated with cont. phase)<br>2. iso-amyl alcohol (saturated with cont. phase) |
| Flow rate range of $u_d$, cm/s | $0.0776 < u_d < 0.767$; $5.68 < u_N < 56.2$ | $0 < u_d < 1.413$; $0 < u_N < 110$ cm/s |
| Continuous phase | Laboratory distilled water (saturated with MIBK) | Laboratory distilled water (saturated with the respective disp. phase liquid) |
| Flow rate range of $u_c$, cm/s | $0 < u_c < 0.25$ | $0.258 < u_c < 0.774$ |
| Tracer dye (nontransferable to the other phase) | Concentrated solution of the organic dye Garnet GBC Base dissolved in MIBK phase | 1. 'Durazol Blue 4 GS' in water — for use with MIBK as disp. phase<br>2. 'Durazol Grey' in water — for use with isoamyl alcohol as disp. phase |

color was noticed in the dispersed phase outlet.

The dye injection procedure was repeated three times for each set of dispersed and continuous phase flow rates in order to check the reproducibility of data. The experiments covered a range of flow rates limited by the maximum flow rate the glass nozzles of the present experimental setup could provide.

Holdup measurements were made at the end of each run by shutting off the inlet and exit valves and by allowing the dispersed phase to settle at the top of the column which was measured by the usual displacement method.

*Tracer.* A strong solution of an organic dye, Garnet GBC Base (chemical name: metanitro orthophenitidine) dissolved in methyl isobutyl ketone (MIBK) nontransferable to the water phase was used. No appreciable change in the interfacial tension was indicated by du Nouy Tensiometer measurements.

The length of the short column was chosen so that the interface could be maintained at least 1 cm above the maximum jetting length that could be encountered. A distance of about 5 cm from the nozzle tip to the interface was found to be satisfactory for all flow rates.

*Photographic Setup For Drop Size Studies.* The photographic arrangement used in the present study was very similar to the one reported by Vedaiyan et al. (1972), with improved lighting by two photo flood lamps in the front of the column area to be photographed. Backlighting through a frosted glass plate was provided by a 200 W lamp in the rear of the column at approximately 30 cm from the column. It gave each drop a dark outline and sharp silhouette against a bright background. A blue solution of an organic dye Victoria Blue dissolved in water kept in a glass tank of rectangular cross section was placed in the path of the light beam entering the rear of the column in order to improve the contrast and also absorb the heat liberated by the rear lamp. Shields were used to eliminate all extraneous lights.

The camera used was a Leica M3 with Visoflex attachment. Visoflex with F3.5 lens enabled macrophotography on an area of 22 × 18 mm. With this special attachment it was possible to obtain photographs exactly in the plane of focus. The droplets in the photographic image were magnified to about one and one-half times the actual drop size. The rear end of the camera was fixed 20.5 cm from the front of the column. The photographed area (focal area) along the vertical plane was about 1 cm from the central axis of the column.

Distortion corrections for the vertical and horizontal axis measurements of the drop photographic images were applied before the actual drop size $d_e$ was determined. The equivalent diameter of single drops $d_e$ and the Sauter mean diameter $d_{vs}$ of the dispersion were calculated by using standard equations, namely

$$d_e = \sqrt[3]{d_1^2 d_2}$$

$$d_{vs} = \frac{\Sigma n d_e^3}{\Sigma n d_e^2}$$

where $d_1$ and $d_2$ are the corrected horizontal and vertical axis lengths of the drops, and $n$ is the total number of drops in the sample.

### Continuous Phase RTD Measurements

The experimental setup is essentially the same as described for RTD studies of dispersed phase. In this case only the long column was used, since the RTD for short column remained practically the same, exhibiting plug flow behavior for all flow rate conditions.

Various dyes were tried before a proper choice was made. Durazol Blue 4 GS was found suitable for the water phase with MIBK phase as the dispersed liquid. Durazol Grey was found to be suited for dyeing of the water phase with iso-amyl alcohol as the dispersed phase. The quantity of the saturated solution of the dye in water phase required for pulse input was 10 cm$^3$ per experiment, having an initial concentration of 4% (10 g dye in 250 cm$^3$ water).

*Column Operation.* The spray column was operated in the normal manner with dispersed packing of drops. At steady operation of the column, the actual flow rates of

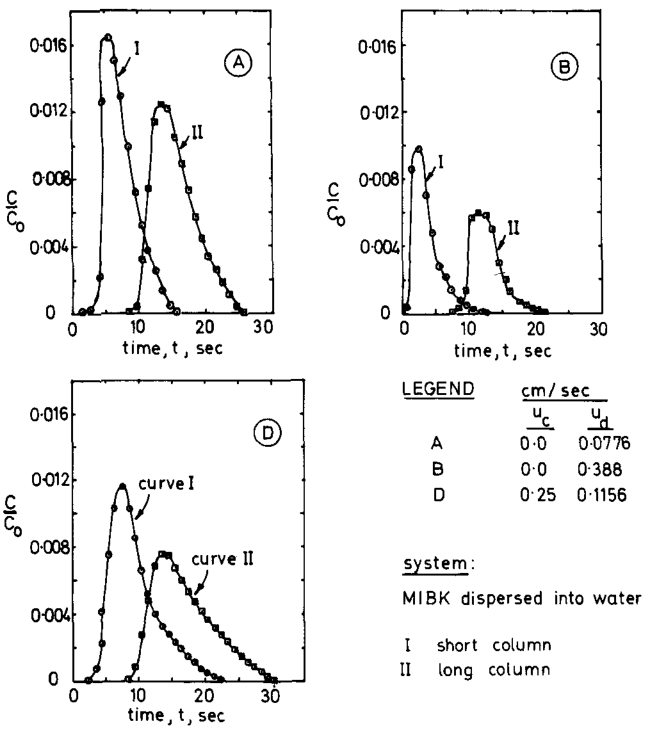

**Fig. 2. Typical concentration-time curves for dispersed phase RTD.**

the two phases were measured. The tracer dye solution of 10 $cm^3$ was shot into the continuous phase inlet distributor through a syringe. The collection of samples was stopped when there was no trace of color in the continuous phase exit stream. The samples were analyzed for their dye concentrations by using a Hellinge Bio-Colorimeter with microplungers. To obtain concordant results and to check the reproducibility of data, three dye injection trials were made for each run operating at any given set of flow rates. RTD data were obtained for a wide range of flow rates of the continuous and dispersed phases. The dispersed phase holdup was obtained for all the runs by the displacement method described earlier .

## DETAILED EXPERIMENTAL RESULTS

Results obtained for both the dispersed and the continuous phases are presented in Figures 2 through 11. The RTD results show that the dynamics of each phase are intimately coupled with the other.

### Results from Studies of the Dispersed Phase

Figure 2 presents a typical RTD concentration-time curve for two output locations sampling of the dispersed phase based on 34 data sets in the range of variables noted on Table 2. Each point for the RTD variance $\sigma_d^2$ is given as the average of three trials of dye injections. The calculations of RTD results followed the methods outlined on Table 1.

Figures 3 and 4 show the dispersed phase RTD variance $\sigma_d^2$ and the drop size distribution variance as functions of nozzle velocity. Note the similarity of these two results. Thus, those factors determining the drop size distribution may be the same as those which determine axial mixing in the dispersed phase.

The variance of dispersed phase RTD and the Peclet numbers describing axial mixing were found to be best correlated with dispersed phase holdup rather than with nozzle velocity or any modified form of the Reynolds number $(d_N u_N \rho_d/\mu_d)$ or $(d_{vs}\overline{u}_o \rho_c/\mu_c)$. Figures 5 and 6 give plots of the present data along with those of Letan and Kehat (1969) which are included for comparison.

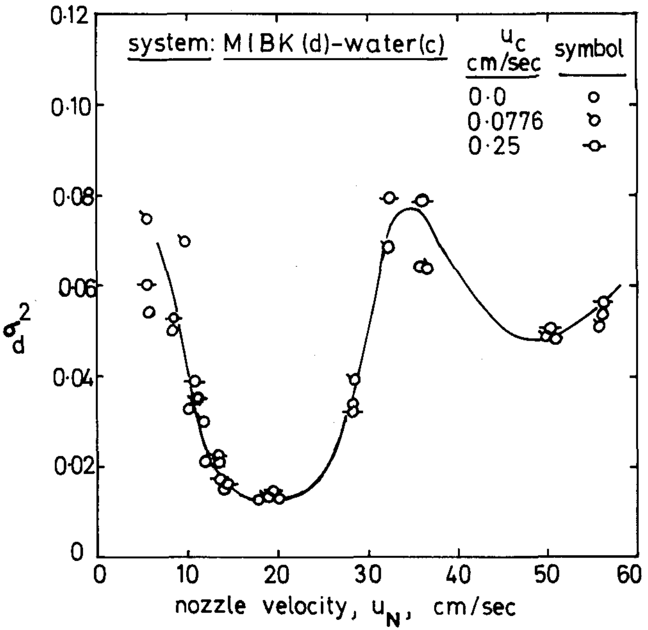

**Fig. 3. Effect of nozzle velocity on RTD variance of dispersed phase.**

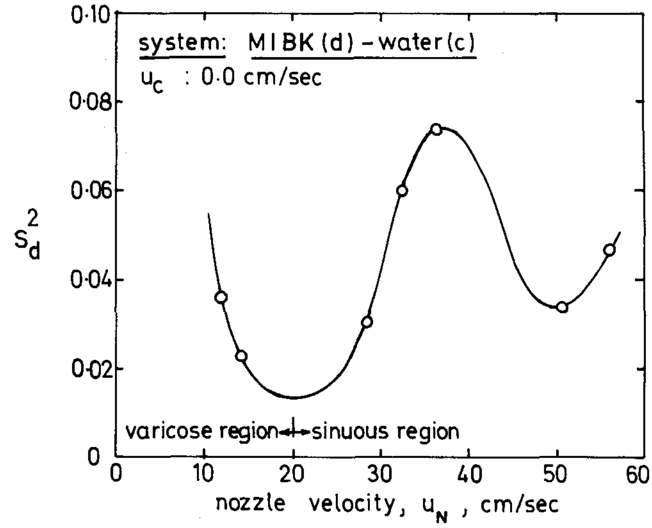

**Fig. 4. Effect of nozzle velocity on the variance of drop size distribution.**

The following equation was found to represent the data of this study with an average deviation of ± 23% and a maximum deviation of 54%:

$$(Pe)_d = \frac{2}{\sigma_d^2} = 21 + \frac{1}{2\,500\,x^2} + 139\left[\exp\left(-\frac{(x-0.025)^2}{7\times10^{-5}}\right) + 0.14\exp\left\{-\frac{(x-0.075)^2}{5.2\times10^{-4}}\right\}\right] \quad (1)$$

### Results from Studies of the Continuous Phase

The RTD results from studies of the continuous phase were found to be of standard form. There remains no fully satisfactory correlation of variance or axial dispersion coefficient for the continuous phase. Former studies correlate existing data (including those of this work) with wide scatter. The following new equation based on the important parameter $u_N$ correlates the present data in the form of a modified continuous phase Peclet number with an average deviation of ± 19% and a maximum deviation of 39%. Thus

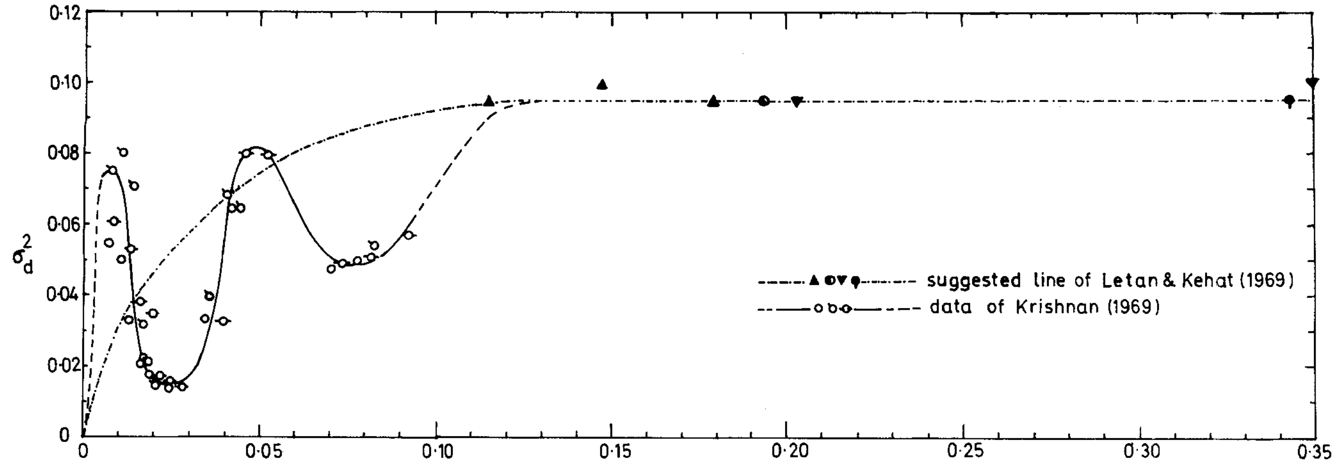

Fig. 5. Effect of holdup on RTD variance of dispersed phase. (T. R. Krishnan, 1969).

$$\frac{u_c d_{vs}}{E_c}\left(\frac{u_d}{u_c}\right)^{0.5} = 0.014 \exp\left[0.0005\left(\frac{d_N u_N \rho_c}{\mu_c}\right)\right] \quad (2)$$

A plot of these data is given in Figure 11. The present data appears to correlate well according to Equation (2). However, data covering a wider range of values of the variables need to be analyzed for a general applicability of Equation (2).

**Studies of the Interaction of Continuous and Dispersed Phases**

The effect of dispersed phase velocity at the nozzle $u_N$ or holdup on the variance of RTD of the continuous phase $\sigma_c^2$ is shown for the MIBK-water system on Figure 8. A similar result was found when an iso-amyl alcohol-water system was used. These results are typical of those observed throughout this study. An increase in $u_c$ at any $u_N$ caused a decrease of $\sigma_c^2$. However, for a given $u_c$, an increase in $u_N$ caused increase of $\sigma_c^2$ to a maximum after which it decreased. The effect of $u_N$ or holdup on the variance of RTD of the dispersed phase $\sigma_d^2$ (see Figure 3) gave the opposite result in that $\sigma_d^2$ decreased first with $u_N$ to a minimum, then increased to a maximum before it decreased again to a second minimum. A similar observation for the variance of drop size distribution of the droplet swarms was observed with $u_N$ as shown on Figure 4.

Figures 3, 4, and 8 indicate a close relationship between $\sigma_c^2$ and $\sigma_d^2$ with respect to nozzle velocity $u_N$. Figure 4 offers an explanation for the above observations in terms of the changing pattern of drop size distribution with increased $u_N$. Note, the first minimum of Figures 3 and 4 and the maximum of Figure 8 correspond to almost identical nozzle velocities, that is, the critical nozzle velocity. The second minimum in Figures 3 and 4 corresponds to identical values for $u_N$ at that point.

## A SUMMARY DISCUSSION OF RESULTS

Curves I and II on Figure 2 represent RTD results for the dispersed phase for the short and long column, respectively. The time displacement of II is, of course, caused by the residence time in the column, and its increasing width and skewness as velocities increase give an indication of the distribution of residence times for different size droplets in the swarm. However, as the dispersed phase flow rate increases, II is influenced by axial mixing, and at very high flow rates a long tail is observed due, apparently, to the presence of large numbers of fine droplets in the dispersion. This condition caused increased difficulty in determining the dye concentration. Material balance studies showed that the amount of dye in this tail section was usually less than 1% of the inlet amount.

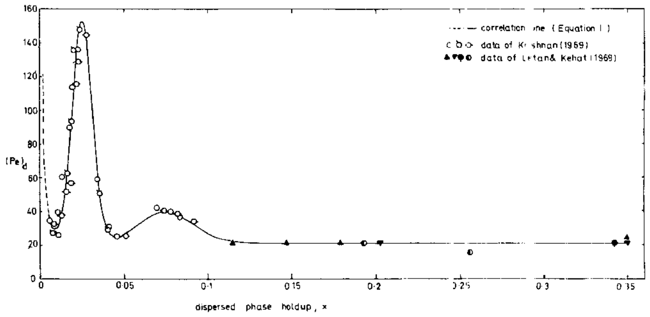

Fig. 6. Correlation of dispersed phase axial mixing data.

Average residence times $\overline{t}_{\text{exp}}$ calculated as shown on Table 2 from flow rate and holdup agreed well with the mean residence time $\overline{t}$ calculated from RTD results. The closed vessel model was used to calculate the continuous phase mean residence time, since a single output location was found sufficient for the RTD experiments.

The work of Vedaiyan et al. (1972, 1974) indicated that the drop size distribution passes through a mono to bi to monomodal distribution as $u_N$ increases. This phenomenon has been explained in the above reference. The result shown on Figure 4 seems consistent with this change in the drop size distribution function. The variation of $E_c$ with $u_c$ as shown on Figure 9 agrees with the observations of Hazlebeck and Geankoplis (1963).

Finally, the interaction of $\sigma_c^2$ and $\sigma_d^2$ with nozzle velocity is worthy of comment. Figures 3, 4, and 8 present the basic result.

At low dispersed phase flow rates, the relatively few large drops present in the column tend to entrain chunks of continuous phase in their wakes. Since the total drop population moving through the continuous phase is small, the motion of the continuous phase does not significantly increase axial dispersion in that phase (see Figure 8). As $u_N$ increases, holdup increases, yielding large numbers of uniform sized drops. This continues to the critical velocity region corresponding to the minimum $\sigma_d^2$ value. Here, all drops move against the direction of flow of the continuous phase with almost identical terminal velocities, each entraining an approximately equal volume of continuous phase in its wake, causing backmixing in the continuous phase. The drop population (holdup) is now larger than at lower flow rates, and their uniform motion through the countercurrently flowing continuous phase results in turbulence of that phase as shown by the maximum value of $\sigma_c^2$.

When $u_N$ is further increased, bimodality in the drop size distribution is observed, and the number of smaller

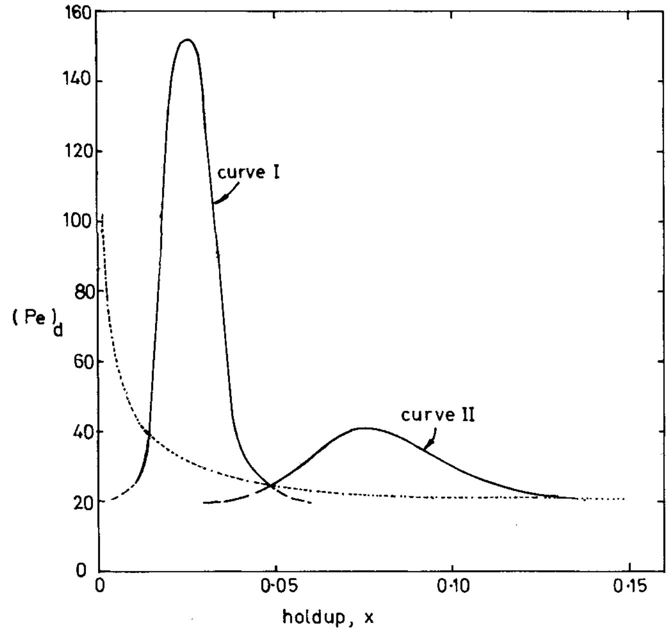

Fig. 7. Interpretation of correlation of *(Pe)ₐ*.

drops in the population increases. Holdup increases. The drop size distribution then becomes nonuniform. Even though the holdup is increased, smaller drops in the ensemble do not entrain much continuous phase. Also, owing to their low terminal velocities, they do not cause extensive mixing of the continuous phase. However, the presence of large numbers of small drops in the crowded swarm tends to keep the continuous phase variance high compared to that at very low holdup of the drop phase.

## CORRELATING EQUATIONS

### For the Dispersed Phase Variance or Peclet Number

The variation of $\sigma_d^2$ with holdup (Figure 5) and of $\sigma_d^2$ with $u_N$ (Figure 3) indicates that $\sigma_d^2$ is correlated best with holdup for the entire set of flow rates rather than with nozzle velocity, orifice Reynolds number $(d_N u_N \rho_d/\mu_d)$, or the modified Reynolds number $(d_{vs}\bar{u}_o\rho_c/\mu_c)$. On Figure 5, the interpolated data of Letan and Kehat (1969) are shown for comparison. (Note that their data on holdup were obtained by interpolation from their plot by assuming a value of 0.35 for holdup at flooding.)

By considering the present dispersed phase RTD data obtained by the two output location method to represent an open vessel, axial mixing Peclet numbers $(u_d L/E_d)$ were obtained by using the relationship on Table 1. These were plotted with holdup as shown on Figure 6. The data of Letan and Kehat (1969) (holdup $< 0.35$) are also shown. Equation (1) is found to correlate the data satisfactorily to a holdup of 0.35. The bimodal character of the correlation plot on Figure 6 may be explained by separating it into two curves as shown on Figure 7. The Peclet number $(Pe)_d$ should show an exponential decrease (see Figure 7) as the holdup is increased. Increased drop population and crowding effects should increase axial mixing as suggested by Letan and Kehat (1969). However, at the varicose region (low holdup, $u_d$), the axial mixing Peclet number values increase owing to near normal distribution of drops with maximum uniformity and uniform velocity of rise up the column. This part relates to the rising side of curve I of Figure 7. As the drop population becomes more nonuniform in the sinuous region, the axial mixing Peclet numbers decrease (see the falling side of curve I, Figure 7). Further increases in nozzle velocity and holdup result in the formation of a bimodal distribution, one part with a large size fraction and another with small size fraction. Note the intersection of curves I and II. $(Pe)_d$ increases again until the fraction attributable to the smaller drops increases to equal that of the larger drops. Note the rising part of curve II of Figure 7.

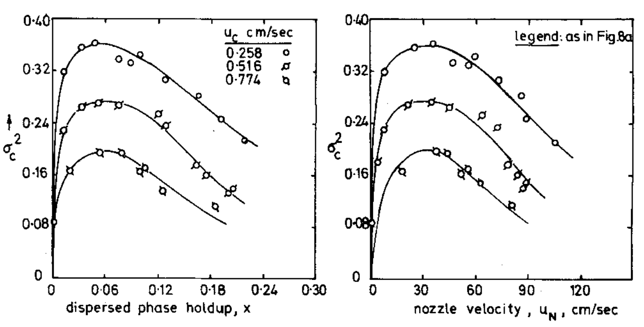

(a) (b)

system: MIBK dispersed into water

Fig. 8. Effect of holdup and nozzle velocity on continuous phase variance.

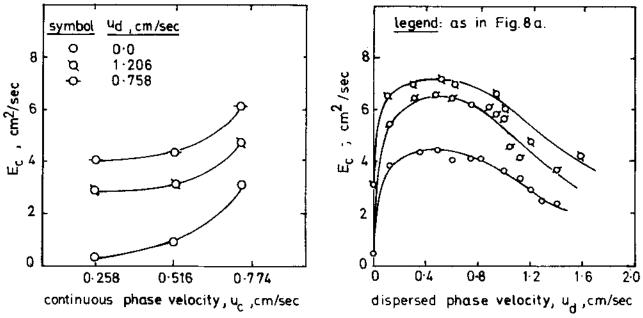

(a) (b)

system: MIBK dispersed into water

Fig. 9. Effect of phase flow rates on $E_c$.

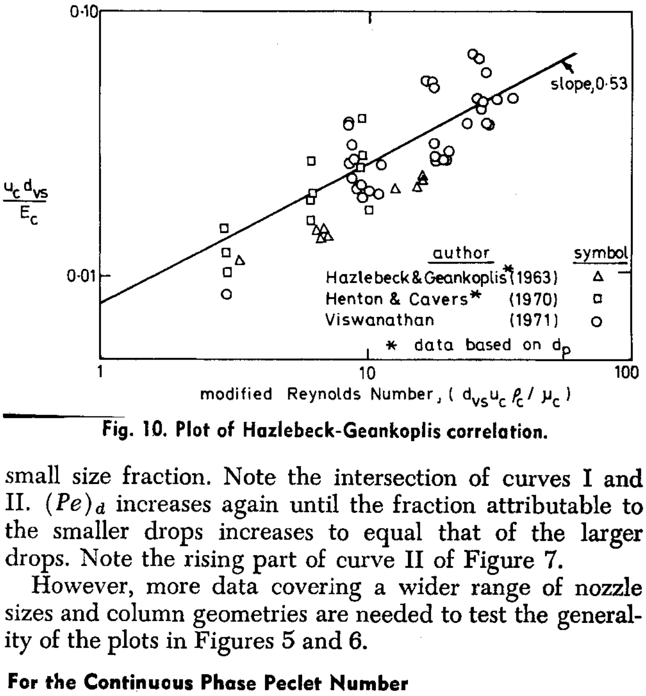

Fig. 10. Plot of Hazlebeck-Geankoplis correlation.

However, more data covering a wider range of nozzle sizes and column geometries are needed to test the generality of the plots in Figures 5 and 6.

### For the Continuous Phase Peclet Number

The following modified forms of relationships were used to correlate the present data, taking into account the computed values of $d_{vs}$ instead of $d_p$, the drop diameter as defined by Hazlebeck and Geankoplis (1963) and Henton and Cavers (1970) in their attempts to correlate the continuous phase RTD data:

$$\frac{u_c d_{vs}}{E_c} = \alpha\left(\frac{d_{vs}\,u_c\,\rho_c}{\mu_c}\right)^n \tag{3}$$

$$\frac{E_c}{d_{vs}\bar{u}_o} = f\left(\frac{d_{vs}\,u_s\,\rho_c}{\mu_c}\right) \tag{4}$$

For the data of the present investigation, the values of the

TABLE 3. RANGE OF VARIABLES FOR HAZLEBECK—GEANKOPLIS CORRELATION

| Author and reference | Range of flow rates, cm/s |  | Range of $(u_c d_{vs}/E_c)$ |
|---|---|---|---|
|  | $u_c$ | $u_d$ |  |
| Hazlebeck and Geankoplis (1963) | 0.080-0.465 | 0.154-0.423 | 0.008-0.023 |
| Henton and Cavers (1970) | 0.080-0.445 | 0.238-1.08 | 0.008-0.042 |
| Present work and Viswanathan (1971) | 0.258-0.774 | 0.0-1.413 | 0.0198-0.067 |

characteristic velocity $\bar{u}_o$ were obtained from experimental holdup, and flow rates were obtained by the following slip velocity:

$$u_s = \frac{u_d}{x} + \frac{u_c}{1-x} = \bar{u}_o(1-x) \tag{5}$$

The Sauter mean drop size $d_{vs}$ was determined by the correlation of Vedaiyan et al. (1974), given by:

$$d_{vs} = 1.59 \left(\frac{\gamma}{\Delta \rho g}\right)^{0.5} \left(\frac{u_N^2}{2gd_N}\right)^{-0.067} \tag{6}$$

The correlation represented by Equation (4) is similar in form to that proposed by Levenspiel and Bischoff (1963) for flow through a packed column and gives a wide band of data almost independent of Reynolds number. The spray column data of this work as well as those reported by Henton and Cavers (1970) fit within this band for a narrow range of Reynolds numbers between 300 and 800.

Equation (3) was found to be a better correlation than Equation (4) for the present data and for those of Hazlebeck and Geankoplis (1963) and Henton and Cavers (1970). However, this correlation is still found to be unsatisfactory. A plot of all data is shown on Figure 10. The range of variables of these data for Figure 10 is indicated on Table 3.

### Proposed Correlation

The present analysis of $\sigma_c^2$ indicates that any attempt at correlating the axial mixing Peclet numbers $(Pe)_c$ must take into account the dispersed phase velocity at the nozzle $u_N$ and the effect of phase flow rates $u_c$ and $u_d$ on $(Pe)_c$. Hence, on analysis of the present data in terms of a modified Peclet number, $u_c d_{vs}/E_c$, phase flow rate ratio, and nozzle Reynolds number showed that Equation (2) did fit the data satisfactorily with an average deviation of ± 19% and a maximum deviation of 39%.

## NOTATION

$C(t)$ = concentration of tracer dye at the output location at any time $t$

$C_o$ = concentration of tracer dye at input location

$d_e$ = equivalent drop diameter, cm

$d_N$ = diameter of nozzle of the distributor, cm

$d_T$ = column diameter, cm

$d_{vs}$ = volume-surface drop diameter or Sauter mean, cm

$E$ = axial dispersion coefficient, cm$^2$/s

$g$ = acceleration due to gravity, cm/s$^2$

$L$ = effective column length, cm

$Pe$ = Peclet number, $(uL/E)$ dimensionless

$(Pe)_c$ = modified Peclet number for the continuous phase, $(u_c d_{vs}/E_c)$ dimensionless

$Re$ = Reynolds number

$S_d^2$ = variance of drop size distribution, cm$^2$

$t$ = time, s

$\bar{t}$ = mean residence time, s

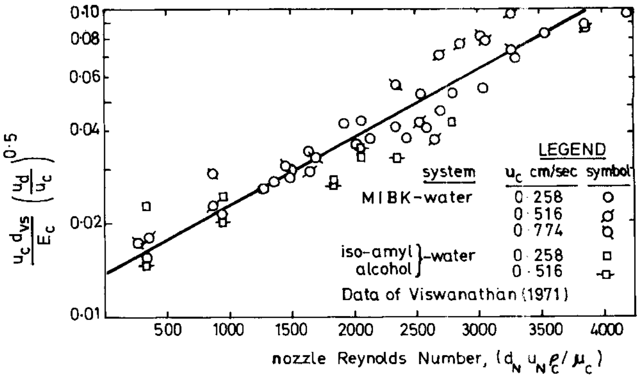

Fig. 11. Correlation of continuous phase axial mixing data.

$u$ = superficial velocity based on column cross section, cm/s

$u_N$ = velocity of dispersed phase at the nozzle, cm/s

$\bar{u}_o$ = characteristic velocity of droplet swarm, cm/s

$u_s$ = slip velocity, cm/s [Equation (6)]

$x$ = holdup of the dispersed phase, fraction

**Greek Letters**

$\gamma$ = interfacial tension, dyne/cm

$\mu$ = viscosity, centipoise

$\mu_t$ = first moment of RTD, s

$\sigma_t^2$ = second moment of RTD, s$^2$

$\sigma^2$ = variance of RTD, s$^2$

$\rho$ = density, g/cm$^3$

**Subscripts**

$c$ = continuous phase

$d$ = dispersed phase

exp = experimental

$N$ = at the nozzle

## LITERATURE CITED

Hazlebeck, D. E., and C. J. Geankoplis, "Axial Dispersion in Spray Type Extraction Tower," *Ind. Eng. Chem. Fundamentals*, **2**, 310 (1963).

Henton, J. E., and S. D. Cavers, "Continous Phase Axial Dispersion in Liquid-Liquid Spray Towers," *ibid.*, **9**, 384 (1970).

Henton, J. E., L. W. Fish, and S. D. Cavers, "Liquid-Liquid Spray Towers, Continuous Phase Peclet Numbers," *ibid.*, **12**, 365 (1973).

Kreager, R. M., and C. J. Geankoplis, "Effect of Tower Height in Solvent Extraction Towers," *Ind. Eng. Chem.*, **45**, 2156 (1953).

Krishnan, T. R., "Studies of Dispersed Phase Residence Time Distribution in Spray Column," M. Tech. thesis, University of Madras, India (1969).

Letan, R., and E. Kehat, "The Temperature Jump at the Inlet of the Continuous Phase in a Spray Column Heat Exchanger," *AIChE J.*, **14**, 831 (1968).

——————, "Residence Time Distribution of the Dispersed Phase in a Spray Column," *ibid.*, **15**, 4 (1969).

Levenspiel, O., *Chemical Reaction Engineering*, 2 ed., Chapt. 9, pp. 253-315, Wiley, New York (1972).

———, and K. B. Bischoff, *Advances in Chemical Engineering*, Vol. 4, pp. 95-198, Academic Press, New York (1963),

Mixon, F. O., D. R. Whitaker, and J. C. Orcutt, "Axial Dispersion and Heat Transfer in Liquid-Liquid Spray Towers," *AIChE J.*, 13, 21 (1967).

Vedaiyan, S., T. E. Degaleesan, G. S. Laddha, and H. E. Hoelscher, "Some Performance Characteristics of Spray Columns," *ibid.*, **18**, 161 (1972).

Vedaiyan, S., T. E. Degaleesan, and G. S. Laddha, "Mean Drop Size and Characteristic Velocity of Droplet Swarms in Spray Columns," *India J. Technol.*, **12**, 135 (1974).

Viswanathan, S., "Studies of Continuous Phase Residence Times in Spray Column," M. Tech. Thesis, University of Madras, India (1971).

*Manuscript received May 9, 1975; revision received October 8, and accepted December 18, 1975.*